EXPERIMENTAL ANALYSES ON IMPACT-INDUCED DAMAGE IN CFRP LAMINATED COMPOSITES WITH SCANNED IMAGE MICROSCOPY

Chiaki Miyasaka[1], Hideaki Kasano[2] and Bernhard R. Tittmann[1]

[1]Department of Engineering Science and Mechanics. The Pennsylvania State University at University Park, Pennsylvania, USA

[2]Department of Mechanical Engineering, Takushoku University, Tatemach 815-1, Hachioji, Tokyo, Japan

Introduction

The impact-induced damage is the most serious type of damage for carbon fiber reinforced composites [1]. In particular, delamination caused by impact loading is known to produce significant reductions in the residual compression strength of carbon fiber reinforced plastic (hereinafter called simply "CFRP") laminated composites. This is a major problem associated with the structural integrity of composite compression components. Much effort has therefore been devoted to the study of the effects of impact-induced damage on the load-bearing capacities of these components in the past 30 years [2-6]. In the course of these studies, attempts have also been made to investigate the damage mechanisms [7-9]. However, only a few detailed studies have been reported on the damage initiation and propagation mechanisms of the CFRP laminated composites, and more work is still required to better understand them. This article reports the results of microscopic examinations of delaminations and transverse cracks detected with scanned image microscopy, from which the initiation and propagation mechanisms of the impact-induced damage were discussed.

Experimental

Materials

The test specimens studied were manufactured from pre-impregnated sheets of KASEl Fiberite HYEJ12. The tensile strength of the carbon fibers in the uni-directional prepreg is in the range of 4.22~4.27GPa and the Young's modulus 231~233GPa. These prepregs are layered up to 22 plies in the stacking sequence of $[0_6/\theta_{10}/0_6]$, where θ denotes the angle of fiber orientation inclined to a longitudinal direction 0 degree of the laminate panels. The dimensions of the laminate test specimens were 180.0mm by 100.0mm with an average thickness of 2.8mm.

Apparatus and Procedure

Impact tests were performed with an air-gun type of apparatus. Air was bled from a supply line into a cylindrical reservoir. Two steel balls, 5.0mm and 10.0mm in diameter, were used as the impactors. The specimens were impacted under two different test conditions. First, steel balls were propelled at the velocity of 60 m/s, with the diameter and weight of the balls chosen to be 5.0mm, 0.5g, 10.0mm, and 4.1g respectively. Second, a 5.0mm-diameter steel ball was accelerated at a velocity of 90.0m/s, and a 10.0mm steel ball at 30.0m/s, which produced the same kinetic energy, *i.e.*, the same impact energy of two Joules.

Results and Discussion

The impact damaged specimens were inspected with scanned image microscopy (*i.e.*, Scanning Acoustic Microscopy: SAM, and Scanning Electron Microscopy: SEM). Interface A was between the 6th and 7th plies, and interface B between the 16th and 17 plies, at which major changes in the fiber orientation occurs. The former is located nearer to the front surface (impacted surface) of the specimen and the latter to the back surface (opposite the impacted surface). Figure 1 shows typical delamination patterns of the test specimens impacted by the 5.0mm diameter steel ball at a velocity of 60.0m/s. The damage zones have a characteristic two-lobed shape, long in the preferred directions, *i.e.*, at interface A, extended mainly in the 90-deg ply direction, while at interface B, in the 0-deg ply direction. The damage was confined locally to the areas centered at the impact location, which suggests that the delamination damage was due to the bending-induced stresses. The effects of ply angle θ on the delamination areas are shown in Figure 2 for the 5.0mm steel balls. The delamination area increases with an increased ply angle θ, and the increasing rate is remarkably higher at interface B than at interface A. The delamination areas are also related to the size of steel balls. The 10.0mm steel ball exhibited more increase in delamination area than the 5.0mm ball when impacted at the same velocity. If the impact energies are the same for each steel ball, a smaller size impactor with higher velocity tends to produce greater delamination damage. The delamination area ratio at interface A is higher than that at interface B. and it should be noted that the averages for the three specimens were very close to the values calculated from V_5/V_{10} (=2.9) and $\sqrt{V_5/V_{10}}$ (=1.7), respectively.

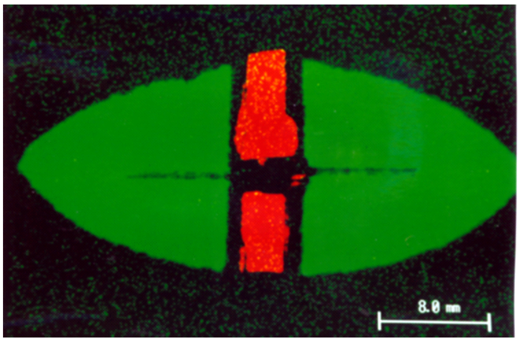

Fig. 1 Superimposed SAM C-scan images (pulse-wave-mode) showing delaminations at interfaces A and B. Frequency: 30 MHz

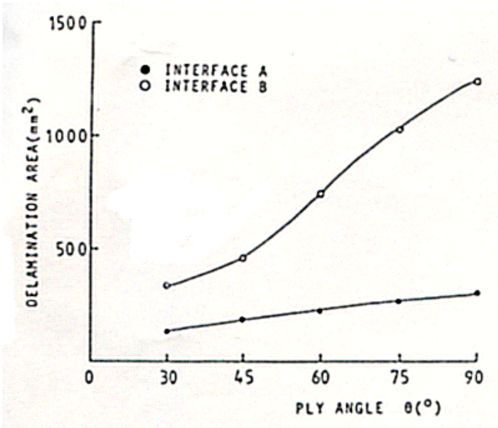

Fig. 2 Delamination area vs. ply angle

To further examine the interior damage, the impacted specimens were cross-sectioned at different locations and inspected using the SEM. The horizontal cracks correspond to the delamination and therefore it can be concluded that small delaminations occurred in the specimens as well as two distinct delaminations at interface A and B inspected by SEM.

Conclusions

The interior damage was characterized by delaminations and transverse cracks. The delaminations were detected clearly at two distinct interfaces, at which a major change in the ply angles occurred. The transverse cracks were observed through the specimen thickness in the cross sections.

The damage zones have a characteristic two-lobed shape, long in the θ-deg ply direction at interface A (nearer to the impacted surface), while in the 0-deg ply direction at interface B (nearer to the back surface opposite the impacted surface).

The transverse cracks can be classified into horizontal, oblique and vertical cracks in the form of matrix cracks or fiber/matrix debondings. Horizontal cracks parallel to the specimen surfaces were found to correspond to the delamination damage. Oblique cracks detected mainly between interface A and B, and between interface A and the impacted surface, were more or less associated with the delamination onset at interface A. Vertical cracks were detected mainly between interface B and the back surface, and they were supposed to be greatly associated with the delamination onset at interface B.

A smaller size impactor with higher velocity tends to produce greater delamination area and more transverse cracks when impacted at the same kinetic energy, while a larger size impactor exhibits more increase in delamination area when impacted at the same velocity.

References

1. Challenger, K.D., The Damage Tolerance of Carbon Fiber Reinforced Composites-A Workshop Summary, Composite Structures, Vol. 6, pp. 295-318, 1986.
2. Starnes, J.H., Jr., Rhodes, M.D., & Williams, J.G., Effect of Impact Damage and Holes on the Compressive Strength of a Graphite/Epoxy Laminate, ASTM STP696, 1979, pp. 145-171.
3. Sharma, A. V., Low-Velocity Impact Tests on Fibrous Composite Sandwich Structures, ASTM STP734, 1981, pp. 54-70.
4. Labor, J. D., Impact Damage Effects on the Strength of Advanced Composites, ASTM STP696, 1979, pp. 172-184.
5. Williams, J. D., Rhodes, M. D., Effect of Resin on Impact Damage Tolerance of Graphite/Epoxy Laminates, ASTM STP787, 1982, pp. 450-480.
6. Sharma, A. V., Effect of Specimen Size on the Buckling Behavior of Laminated Composites Subjected to Low-Velocity Impact, ASTM STP808, 1983, pp. 140-154.
7. Rhodes, M. D., Williams, J. G., Starnes, J. H., Jr., Low Velocity Impact Damage in Graphite-Fiber Reinforced Epoxy Laminates, Polymer Composites, Vol. 2, No. 1, pp. 36-44, 1981.
8. Takeda, N., Sierakowski, R. L., & Marvern, L. E., Microscopic Observations of Cross-Sections of Impacted Composites Laminates, Composite Technology Review, Vol. 41, No. 1, pp. 40-44, 1982.
9. Malvern, L. E., Sierakowski, R. L., & Ross, C. A., Impact Failure Mechanisms in Fiber Reinforced Composite Plates, Proc. IUTAM, 1977, pp. 24-27.